

# UC Davis

## UC Davis Previously Published Works

### Title

A role for Gle1, a regulator of DEAD-box RNA helicases, at centrosomes and basal bodies.

### Permalink

<https://escholarship.org/uc/item/7t9135t9>

### Journal

Molecular biology of the cell, 28(1)

### ISSN

1059-1524

### Authors

Jao, Li-En  
Akef, Abdalla  
Wente, Susan R

### Publication Date

2017

### DOI

10.1091/mbc.e16-09-0675

Peer reviewed

# A role for Gle1, a regulator of DEAD-box RNA helicases, at centrosomes and basal bodies

Li-En Jao<sup>†,\*</sup>, Abdalla Akef, and Susan R. Wentz

Department of Cell and Developmental Biology, Vanderbilt University School of Medicine, Nashville, TN 37240

**ABSTRACT** Control of organellar assembly and function is critical to eukaryotic homeostasis and survival. Gle1 is a highly conserved regulator of RNA-dependent DEAD-box ATPase proteins, with critical roles in both mRNA export and translation. In addition to its well-defined interaction with nuclear pore complexes, here we find that Gle1 is enriched at the centrosome and basal body. Gle1 assembles into the toroid-shaped pericentriolar material around the mother centriole. Reduced Gle1 levels are correlated with decreased pericentrin localization at the centrosome and microtubule organization defects. Of importance, these alterations in centrosome integrity do not result from loss of mRNA export. Examination of the Kupffer's vesicle in Gle1-depleted zebrafish revealed compromised ciliary beating and developmental defects. We propose that Gle1 assembly into the pericentriolar material positions the DEAD-box protein regulator to function in localized mRNA metabolism required for proper centrosome function.

## Monitoring Editor

Karsten Weis  
ETH Zurich

Received: Sep 26, 2016

Revised: Oct 31, 2016

Accepted: Nov 2, 2016

## INTRODUCTION

The centrosome and its related organelle cilium coordinate critical signals that regulate cell function and influence development. As the major microtubule-organizing center (MTOC) in animal cells, the centrosome influences cell shape, polarity, and motility by regulating microtubule (MT) organization (Doxsey, 2001; Bornens, 2002; Nigg, 2002). The centrosome consists of a pair of centrioles and the associated protein-dense pericentriolar material (PCM). Unlike the centriole, which shows a rigid, ninefold-symmetric cylindrical structure of MTs, the PCM displays as an amorphous structure under the electron microscope (Rieder and Borisy, 1982). Recent advances in superresolution microscopy reveal that individual PCM components adopt a higher-order organization around centrioles (Fu and Glover,

2012; Lawo *et al.*, 2012; Mennella *et al.*, 2012; Sonnen *et al.*, 2012). Understanding how the structure and function of the PCM are controlled is critical to dissecting the roles of centrosomes in different biological and pathological contexts.

The centrosome is not a static organelle. As cells enter mitosis, centrosomes drastically increase in size through the expansion of the PCM (known as centrosome maturation). The PCM plays a critical role in mitosis, as it nucleates MTs (Boveri, 1900; Gould and Borisy, 1977) and enables centrosomes to become robust MTOCs for organization of the spindle apparatus. The PCM is also involved in centriole duplication (Dammermann *et al.*, 2004; Loncarek *et al.*, 2008) and basal body formation (Martinez-Campos *et al.*, 2004; Moser *et al.*, 2010). In differentiated cells, the "mother" centriole (the older of the pair) can transform into a basal body, from which two types of MT structures—motile and primary (nonmotile) cilia—nucleate and protrude from the cell surface. Nonmotile primary cilia are present in nearly all cells and are believed to act as a sensory "antenna" for the cell. Motile cilia exhibit a rhythmic beating motion and are restricted to certain populations of cells, where they serve a number of functions ranging from the simple movement of extracellular debris to the complex process that establishes proper left-right asymmetry in vertebrate body planes.

In our prior studies, we found that inositol 1,3,4,5,6-pentakisphosphate 2-kinase (Ipk1) is enriched at the centrosome and basal body in zebrafish embryos, allowing localized production of inositol hexakisphosphate (IP<sub>6</sub>) required for proper ciliary beating and length maintenance (Sarmah *et al.*, 2007). Depletion of Ipk1 randomizes

This article was published online ahead of print in MBoC in Press (<http://www.molbiolcell.org/cgi/doi/10.1091/mbc.E16-09-0675>) on November 9, 2016.

L.J. and S.R.W. conceived and designed the experiments; L.J. and A.A. performed the experiments; L.J., A.A., and S.R.W. analyzed the data; L.J. and S.R.W. wrote the manuscript.

<sup>†</sup>Present address: Department of Cell Biology and Human Anatomy, School of Medicine, University of California, Davis, Davis, CA 95616-5270.

\*Address correspondence to: Li-En Jao ([ljao@ucdavis.edu](mailto:ljao@ucdavis.edu)).

Abbreviations used: MT, microtubule; PCM, pericentriolar material; PCNT, pericentrin.

© 2017 Jao *et al.* This article is distributed by The American Society for Cell Biology under license from the author(s). Two months after publication it is available to the public under an Attribution–Noncommercial–Share Alike 3.0 Unported Creative Commons License (<http://creativecommons.org/licenses/by-nc-sa/3.0>).

"ASCB®," "The American Society for Cell Biology®," and "Molecular Biology of the Cell®" are registered trademarks of The American Society for Cell Biology.

both left–right patterning and the asymmetry of normal heart tube placement, with  $\text{Ca}^{2+}$  fluxes also altered at the Kupffer's vesicle, an organ implicated in axial specification during early development (Sarmah *et al.*, 2005). Ipk1 also distinctly marks the nuclear envelope (NE) in budding yeast and plants (York *et al.*, 1999; Lee *et al.*, 2015) in close proximity to Gle1, a well-characterized conserved  $\text{IP}_6$ -binding protein (Alcazar-Roman *et al.*, 2006, 2010; Weirich *et al.*, 2006; Lee *et al.*, 2015).

Gle1 is a multifunctional essential regulator of DEAD-box proteins (Dbps) throughout multiple phases of the mRNA life cycle, including mRNA export, translation, and stress granule formation. Gle1 function has been most carefully dissected at the site of nucleocytoplasmic transport: nuclear pore complexes (NPCs) embedded in the NE. At the cytoplasmic face of NPCs,  $\text{IP}_6$ -bound Gle1 stimulates the RNA-dependent ATPase activity of Dbp5 (Alcazar-Roman *et al.*, 2006; Weirich *et al.*, 2006) to trigger the “remodeling” of mRNA-ribonucleoprotein particles (mRNPs) and confer directionality on mRNA export through NPCs (Alcazar-Roman *et al.*, 2006; Weirich *et al.*, 2006; Tran *et al.*, 2007; Montpetit *et al.*, 2011). Gle1 also regulates efficient translation initiation and termination through the DEAD-box proteins Ded1 (the *Saccharomyces cerevisiae* orthologue of human DDX3) and Dbp5, respectively (Bolger *et al.*, 2008; Bolger and Went, 2011). Under stress conditions, human Gle1 is localized to stress granules, where it interacts with DDX3 and modulates the distribution of mRNAs between the states of active and repressed translation (Aditi *et al.*, 2015). The recruitment and specificity of Gle1 function appear to be dictated by localized interaction partners: at NPCs, by interaction with specific NPC proteins (nucleoporins [Nups]; Rayala *et al.*, 2004; Kendirgi *et al.*, 2005), and in translation initiation by associating with eIF3 (Bolger *et al.*, 2008).

There are also established connections between developmental diseases and misregulation of Gle1 function (Nousiainen *et al.*, 2008; Kaneb *et al.*, 2015). Mutations in *GLE1* have been causally linked to a human congenital disorder, lethal congenital contracture syndrome 1 (LCCS1) (Nousiainen *et al.*, 2008). In a zebrafish model of LCCS1, we showed that apoptosis of organ precursors, including neural precursors, contributes to the pathogenesis of LCCS1 (Jao *et al.*, 2012). Different *GLE1* mutations have also been linked to a familial form of amyotrophic lateral sclerosis, with a disease mechanism apparently distinct from that of LCCS1, in which haploinsufficiency potentially affects the disease pathology in these patients (Kaneb *et al.*, 2015).

Here we report that Gle1 is localized to centrosomes and basal bodies and is a novel PCM component that forms toroid-like organization around the outer layer of the PCM. Down-regulation of Gle1 activity leads to defects in both centrosome integrity and ciliary motility. These are reflected in the loss of a major PCM component, pericentrin (PCNT), from the centrosome and compromises in centrosomal MT nucleation, as well as a defect in the asymmetry of heart looping. Of importance, the centrosomal perturbations caused by Gle1 deficiency are independent of defects in mRNA export. We propose that Gle1-regulated mRNA metabolism at the centrosome mediates proper assembly and function of this essential organelle and that impaired Gle1 function at the centrosome/basal body potentially contributes to the pathogenesis of human disorders linked to *GLE1* mutations.

## RESULTS

### Gle1 localizes to the mother centriole and basal body

Our prior studies show that human Gle1 shuttles between the nucleus and cytoplasm with steady-state localization at NPCs (Kendirgi *et al.*, 2003) and is also at cytoplasmic stress granules under

stress conditions (Aditi *et al.*, 2015). On the basis of the requirement for  $\text{IP}_6$  at basal bodies of cilia in zebrafish (Sarmah *et al.*, 2005, 2007), we hypothesized that Gle1 also plays a role at this essential organelle. We therefore used confocal fluorescence microscopy to examine the localizations of Gle1 and centrosomal components in zebrafish (Figure 1A) and human hTERT-immortalized retinal pigment epithelial cells (RPE-1; Figure 1B). Enhanced green fluorescent protein (eGFP)–hGle1 fluorescence was significantly coenriched with Cetn4–Tag red fluorescent protein (RFP) at centrosomes in zebrafish (Figure 1A, arrowhead) (Of note, with mosaic labeling, not all of the cilia are labeled with both GFP and RFP.) Moreover, endogenous Gle1 was also concentrated at basal bodies and centrosomes in RPE-1 cells (Figure 1B), as detected by respective localization at the base of the acetylated tubulin-positive cilium and overlapping with PCNT in all centrosomes examined.

To further elucidate the centrosomal association of Gle1 at different cell cycle stages, we examined Gle1 localization in CETN-GFP RPE-1 cells, in which the intensity and number of GFP-tagged

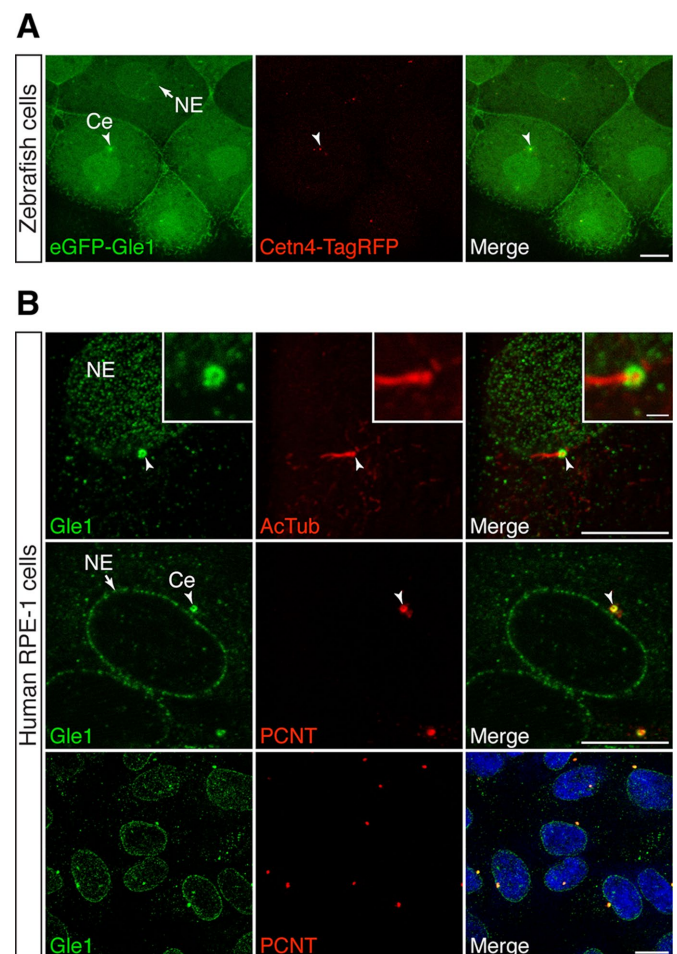


**FIGURE 1:** Gle1 is localized to the centrosome and basal body. (A) eGFP-tagged human Gle1 and Cetn4-TagRFP were transiently expressed from the injected RNA in the cells of dome-stage zebrafish embryos. eGFP-Gle1 localized to the NE (arrow) and the centrosome (Ce; arrowhead). (B) Confocal images of serum-starved human RPE-1 cells stained with antibodies against Gle1 and acetylated tubulin (AcTub; top) or Gle1 and PCNT (middle and bottom). Endogenous Gle1 localized to the ciliary base (top; arrowhead) and the centrosome (middle and bottom; arrowhead) as well as to NE (arrow). Scale bars: 10  $\mu\text{m}$  (main images), 1  $\mu\text{m}$  (insets).

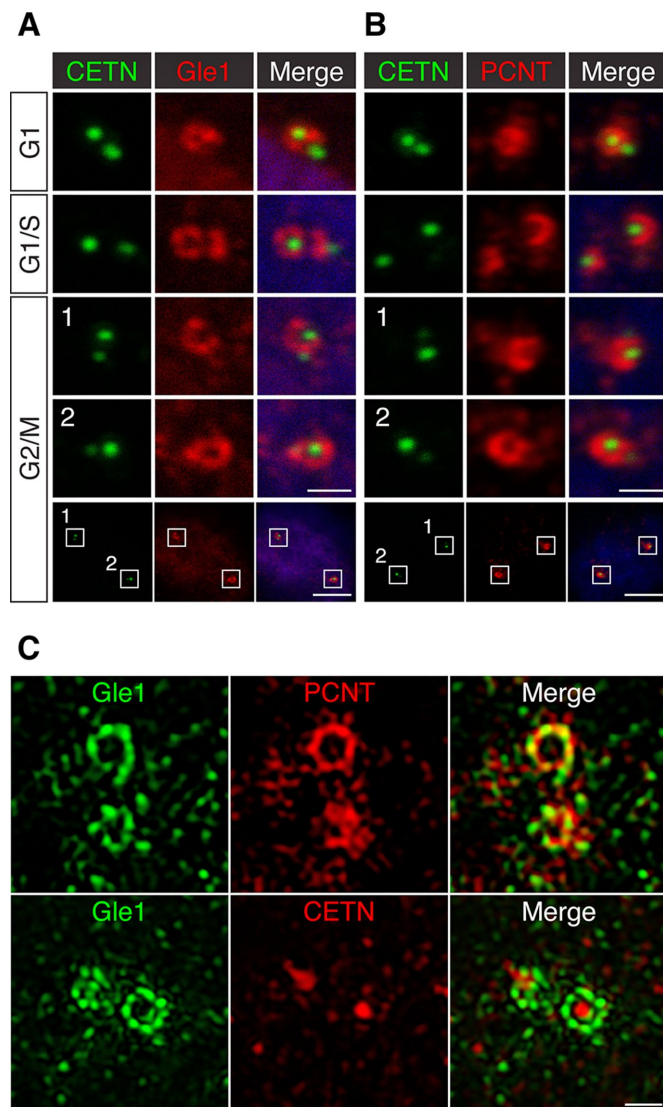


**FIGURE 2:** Gle1 is enriched around the mother centriole and intercalated with PCNT. (A, B) Confocal images of CETN-GFP RPE-1 cells stained with antibodies against Gle1 (A) or PCNT (B) show that Gle1 and PCNT are predominantly localized around the mother centriole at different cell cycle stages. (C) 3D-SIM images of interphase human RPE-1 cells stained with antibodies to Gle1 and PCNT (top) or Gle1 and CETN (bottom). The PCNT antibody recognizes the N-terminal portion of PCNT. Scale bars, 1  $\mu$ m (A, B, all but bottom), 5  $\mu$ m (A, B, bottom), 0.5  $\mu$ m (C).

centriolar distal lumen protein CETN foci are a reflection of cell cycle stages (Loncarek *et al.*, 2008). In G1 cells, immunofluorescence microscopy showed that Gle1 was predominantly present in one of the centrioles (Figure 2A)—the one with a brighter CETN signal, which in general represents the mother centriole (Loncarek *et al.*, 2008). In late G1/S phase, when the daughter centriole became the new “mother” centriole and two centrioles started to duplicate, the Gle1 signals started to encompass the dimmer, new mother centriole (Figure 2A). In G2/M cells, where there were two pairs of centrioles present, each pair with one mother (brighter) and one newly formed daughter centriole, Gle1 was detected predominantly around the mother centriole (Figure 2A). Similar centrosomal localizations were also observed with a different anti-Gle1 antibody (Supplemental

Figure S1A). This toroid-like distribution pattern of Gle1 around the mother centriole was reminiscent of that for PCM, which is predominantly at the mother centriole (Wang *et al.*, 2011). Indeed, we observed a similar mother centriole–dominant, ring-like distribution pattern for one of the major PCM components, PCNT (Figure 2B). Of interest, Gle1 and PCNT localizations at the mother centriole extensively overlapped (see later discussion).

### Gle1 enriches in the outermost layers of PCM intercalated with PCNT

The PCM-like distribution pattern of Gle1 around the mother centriole raised the possibility that Gle1 is a PCM component. Recent advances in superresolution microscopy reveal that the PCM adopts a layered organization around centrioles (Fu and Glover, 2012; Lawo *et al.*, 2012; Mennella *et al.*, 2012; Sonnen *et al.*, 2012). In interphase, PCM proteins form concentric rings or fibril structures around the centriolar core in human centrosomes (Lawo *et al.*, 2012; Sonnen *et al.*, 2012). To examine the centrosomal Gle1 localization at subdiffraction resolutions, we conducted immunofluorescence with three-dimensional structured illumination microscopy (3D-SIM). As shown in Figure 2C, in RPE-1 cells, Gle1 formed a toroid-like, beads-on-string structure around the mother centriole, reminiscent of several PCM components (Lawo *et al.*, 2012; Sonnen *et al.*, 2012). Of interest, Gle1 toroids adopted distinct density masses that resemble the ninefold symmetry of the centriole. The Gle1 toroids did not completely overlap but instead intercalate with the PCNT signals (Figure 2C) and appeared to be also located at a similar distance from the centriolar core as did the PCNT toroid. This suggested that both Gle1 and PCNT occupied similar domains at the outer layer of the PCM. Similar topological structures of Gle1 were also observed in U-2 OS cells (Supplemental Figure S1B).

### Gle1 is required for the centrosomal localization of PCNT and the formation of subdistal appendages

Because Gle1 localized to a pericentriolar region in close proximity with PCNT, we investigated centrosome organization by examining the localization of PCNT and CETN in control and *GLE1* small interfering RNA (siRNA)–treated RPE-1 cells. Immunoblot analysis showed that the Gle1 level was reduced to ~ 50% in a population of *GLE1* siRNA–treated cells (Figure 3A). By immunofluorescence microscopy in *GLE1*–knockdown cells, PCNT signals at the centrosome were reduced, whereas the CETN levels in the centriolar lumen were not affected (Figure 3B). Thus the centriolar core was not perturbed when Gle1 levels decreased. We also observed that the level of ninein (NIN), a component of the subdistal appendages of the mother centriole, was reduced upon the loss of centrosomal Gle1 (Figure 3B). Together these results indicated that Gle1 is required for proper PCNT positioning in the PCM, as well as for the formation of centriolar structures unique to the mature/mother centriole, such as the subdistal appendage.

### Down-regulation of *GLE1* results in an aberrant MT organization independent of mRNA export defects

PCNT is one of the major PCM components required for anchoring the  $\gamma$ -tubulin ring complex, which templates MT nucleation at the centrosome (Dichtenberg *et al.*, 1998; Moritz *et al.*, 2000; Takahashi *et al.*, 2002; Zimmerman *et al.*, 2004). To determine the functional consequence of diminished PCNT levels at the centrosome upon Gle1 depletion, we tested whether MT nucleation was affected upon *GLE1* knockdown by a MT regrowth assay. RPE-1 cells were chilled on ice for 50 min to completely depolymerize MTs. The cells



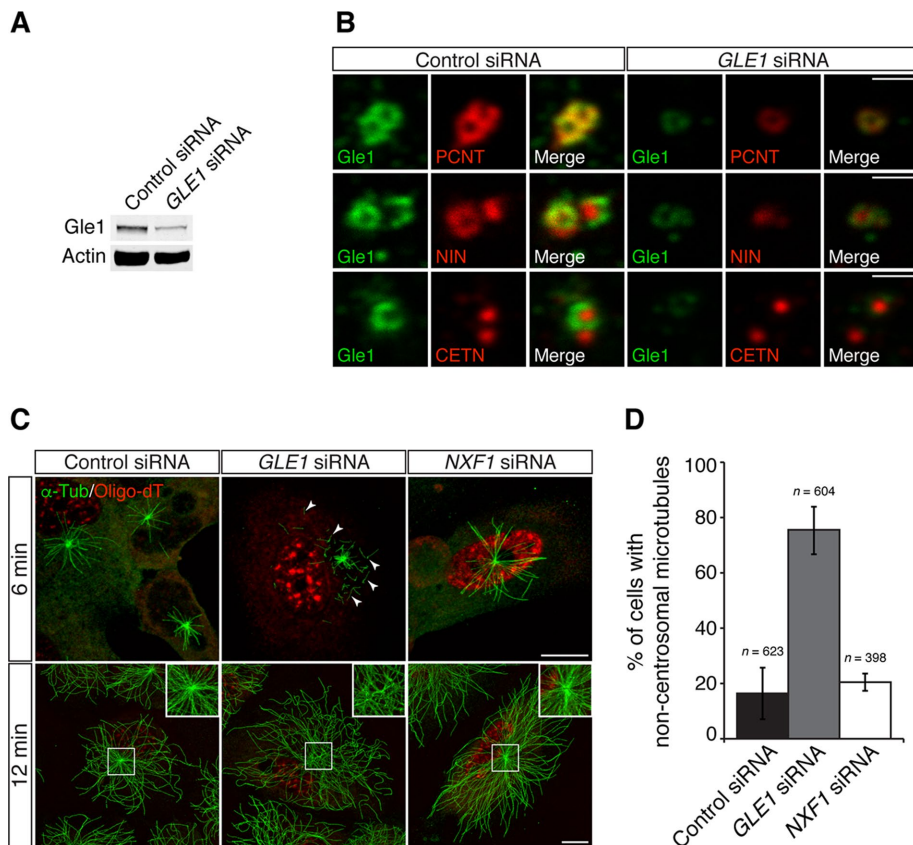


**FIGURE 3:** Gle1 is required for the PCNT, NIN, and MT organization at the centrosome. (A) Total cell lysates of scrambled control siRNA- or *GLE1* siRNA no. 7 (Hs\_GLE1L\_7 FlexiTube siRNA)-transfected cells were analyzed by immunoblotting for Gle1. Actin served as a loading control. A 30- $\mu$ g amount of total protein was loaded per lane. (B) Human RPE-1 cells transfected with scrambled control siRNA or *GLE1* siRNA no. 7 were processed for indirect immunofluorescence microscopy with antibodies against Gle1, as well as against PCNT (top), NIN (middle), or CETN (bottom). (C) Human RPE-1 cells transfected with scrambled control siRNA, *GLE1* siRNA no. 7, or *NXF1* siRNA were subjected to a MT regrowth assay, fixed at the indicated time points, and stained with antibodies to  $\alpha$ -tubulin ( $\alpha$ -Tub), followed by in situ hybridization using Cy3-labeled oligo-dT probes to label poly(A)-containing RNA. In *GLE1*-knockdown cells, increased ectopic cytoplasmic MT nucleation (6 min, *GLE1* siRNA, arrowheads), and few detectable MTs anchored at the centrosome (12 min, *GLE1* siRNA) were observed. (D) Quantification of the MT nucleation events in the MT regrowth assay between RPE-1 cells transfected with scrambled control siRNA, *GLE1* siRNA no. 7, or *NXF1* siRNA. Values are mean  $\pm$  SEM, and *n* is the number of cells analyzed in each condition. Scale bar, 1  $\mu$ m (B), 10  $\mu$ m (C). Using a second *GLE1* siRNA (i.e., *GLE1* siRNA no. 4, Hs\_GLE1L\_4 FlexiTube siRNA) recapitulated the phenotypes (see Supplemental Figure S2).

were then rewarmed to 30°C to induce MT reassembly. At 6 min after rewarming, strong MT asters formed from the centrosome in the control cells. However, in *GLE1* siRNA-treated cells, the MT asters were small (Figure 3C, top). In addition, a majority of the *GLE1* knockdown cells also showed numerous MTs nucleated in the cytoplasm away from the centrosome (Figure 3, C, top, and D). After a longer recovery period (12 min), extensive MT regrowth was observed in both control cells and *GLE1*-knockdown cells. The control cells displayed radially arranged MTs originating mainly at the centrosome. However, in the *GLE1*-knockdown cells, few MTs were focused at the centrosome (Figure 3C, bottom). Similar reduction in centrosomal levels of PCNT and NIN, but not CETN, and defects in MT organization were observed in knockdown cells using two different *GLE1* siRNAs (Supplemental Figure S2 and Figure 3), indicating that these defects are not due to off-target effects of siRNA knockdown.

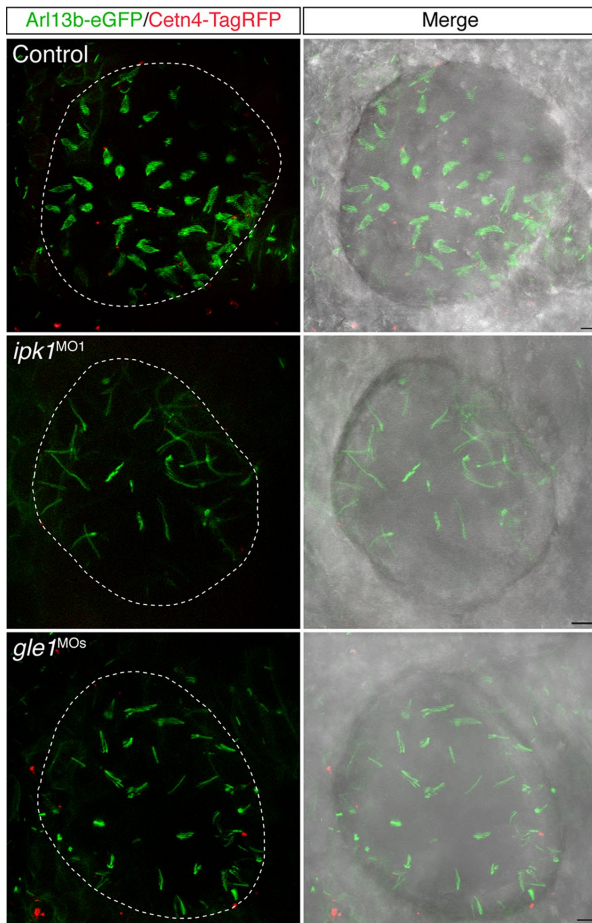
To test whether defects in MT nucleation/anchoring were an indirect consequence of a general inhibition of mRNA export, we analyzed cells with the knockdown of another essential mRNA export factor, *NXF1* (Kang and Cullen, 1999). By in situ hybridization with oligo-dT, nuclear accumulation of poly(A)+ RNA was clearly detected in both *GLE1*- and *NXF1*-knockdown cells, reflecting inhibited nuclear mRNA export (Figure 3C). However, down-regulation of *NXF1* did not phenocopy the MT defects in *GLE1*-knockdown cells (Figure 3C). The percentage of cells with noncentrosomal microtubules was similar in control and *NXF1* siRNA-treated cells (Figure 3D). In contrast, >70% of the *GLE1* siRNA-treated cells showed noncentrosomal microtubules. Thus, independent of its roles in mRNA export, we concluded that Gle1 is uniquely required for organizing PCNT (and likely other PCM components) at the centrosome for proper MT nucleation and anchoring.

### Gle1 knockdown alters ciliary beating and establishment of normal left-right heart looping

Based on the established roles for *IP6* in cilia function, the shared localization of *Ipk1* and Gle1 to basal bodies, and the observation that Gle1 directly binds *IP6* (Alcazar-Roman et al., 2010; Montpetit et al., 2011), we speculated that Gle1 might play a role in cilia function. We used zebrafish to investigate this possibility in a whole-animal model, testing whether ciliary beating in the Kupffer's vesicle (KV) of early embryos was affected upon loss of Gle1 activity using antisense morpholinos (*gle1*<sup>MOs</sup>). Of importance, these *gle1*<sup>MOs</sup> were well characterized in prior studies and did not have off-target effects (Jao et al., 2012). To assess the ciliary beating in vivo, we transiently expressed *Arl13b-eGFP* and *Centrin4* (*Cetn4*)-TagRFP to label the ciliary axonemes and basal bodies, respectively. The beating motion of the GFP-positive motile cilia in the KV rendered a distinct fan-like structure under a fluorescence microscope (Figure 4A, top). To confirm that this imaging strategy was capable of assessing ciliary beating defects, we reduced *Ipk1* activity with a well-characterized antisense morpholino, *ipk1*<sup>MO1</sup>, from our previous study (Sarmah et al., 2005). Consistent with our previous kymography analysis (Sarmah et al., 2005), the stalled ciliary beating defect was readily observed as a distinct loss of the fan-like morphology (Figure 4A, middle). Of interest, the Gle1 knockdown resulted in a ciliary beating defect similar to that observed in *ipk1* morphants (Figure 4A, bottom).

Impaired KV ciliary beating disrupts directional fluid flow within the KV and consequently perturbs left-right (LR) organ patterning, including heart laterality (Essner et al., 2005; Sarmah et al., 2005). We reported heart laterality defects due to impaired KV ciliary beating upon *Ipk1* knockdown (Sarmah et al., 2005, 2007). It is not

**A**



**B**

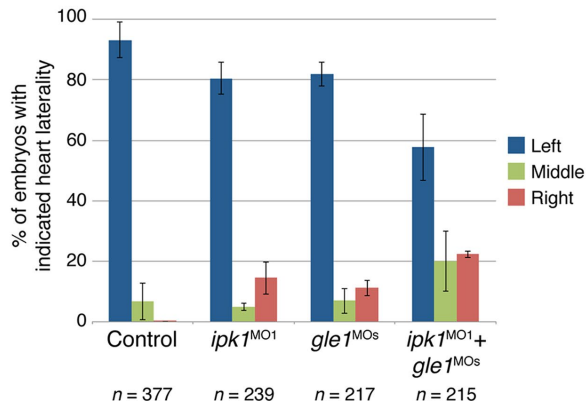


**FIGURE 4:** Depletion of Gle1 reduces ciliary beating and alters left-right asymmetry in zebrafish. (A) The axoneme and the basal body of the cilia were mosaically labeled by Arl13b-eGFP and Cetn4-TagRFP, respectively, in uninjected, *ipk1*<sup>MO1</sup>-injected, or *gle1*<sup>MOs</sup>-injected embryos. Motile cilia in the Kupffer's vesicle were imaged at six- to nine-somite stages from the dorsal side, anterior to the right. Normal ciliary beating is detected by a fan-like morphology in the control. Scale bar, 5  $\mu$ m. (B) Tg(-5.1mnx1:TagRFP) embryos were injected with suboptimal doses of translation-blocking *ipk1* morpholino (*ipk1*<sup>MO1</sup>, 4 ng), a mix of two nonoverlapping translation-blocking *gle1* morpholinos (*gle1*<sup>MOs</sup>, 1.5 ng each), or a combination of both *ipk1*<sup>MO1</sup> and *gle1*<sup>MOs</sup> at the one-cell stage. The direction of the heart looping (TagRFP<sup>+</sup>) was assessed at 60–72 h post fertilization. Three independent injections were performed for each condition. Values are mean  $\pm$  SEM; *n* is the number of embryos analyzed in each condition.

surprising that *gle1* morphants also exhibited heart laterality defects (i.e., the heart looped to the midline or to the right instead of to the left; Figure 4B). Of importance, the laterality defects were exacerbated when *Ipk1* and *Gle1* activities were both knocked down with combined suboptimal doses of both morpholinos (Figure 4B). Thus both *Ipk1* and *Gle1* activities were involved in normal ciliary beating and heart loop left-right asymmetry determination.

## DISCUSSION

Here we report that *Gle1*, a conserved key regulator of several DEAD-box RNA helicases, is localized to the centrosome, forms a toroid-like structure around the mother centriole, and is required for proper PCM composition. We discover an unexpected role of *Gle1* in recruiting a major PCM component, PCNT, and the subdistal appendage protein, NIN, to the mother centriole. We also observe *Gle1* at the basal body and that lack of *Gle1* results in altered ciliary beating and vertebrate left-right body asymmetry.

Analyzing the effects of reduced *Gle1* levels on centrosomal structure and function reveals several specific perturbations. It is striking that cytoplasmic, noncentrosomal MT nucleation increased dramatically upon the loss of *Gle1*. This phenotype resembles the MT regrowth defect of cells with ablated centrosomes (Khodjakov *et al.*, 2000). Both phenotypes are likely a direct consequence of dispersing the  $\gamma$ -tubulin complex, the scaffold for initiating MT nucleation, into the cytoplasm, with the former caused by the disruption of the centrosome itself (Khodjakov *et al.*, 2000) and the latter by the failure of PCNT and PCM assembly at the mother centriole (Figure 3).

In regard to ciliary beating and randomization of heart looping, *Gle1* is also necessary for the assembly of subdistal appendage protein NIN at the centrosome (Figure 3B). Of importance, the subdistal appendage at the mother centriole and the basal foot at the ciliary base form at similar positions along the proximal-distal length of the centriole and share some common components. Thus they have been suggested to have similar etiologies (Anderson, 1972; Kodani *et al.*, 2013). Of importance, basal feet are required for maintaining coordinated ciliary beating (Nakagawa *et al.*, 2001; Kunimoto *et al.*, 2012). Thus, with reduced *Gle1*, the integrity of the subdistal appendage and basal foot is likely compromised, leading to the impaired ciliary motility. Future experiments employing transmission electron microscopy will be able to test this model. Considering our prior discovery of a role for IP<sub>6</sub> production in ciliary beating and length maintenance and regulation of left-right asymmetry (Sarmah *et al.*, 2005, 2007), we further conclude that *Gle1* is at least one of the IP<sub>6</sub> binding targets responsible for the *ipk1* cellular and developmental phenotypes.

How does *Gle1* influence PCNT assembly into the centrosome? There are at least two possible mechanisms. These alternatives are not mutually exclusive. First, *Gle1* might act as a structural scaffold to mediate the interaction of PCNT and other PCM components at the mother centriole. Like many centrosomal proteins, *Gle1* also contains a coiled-coil domain, which is required for its self-association and mRNA export function at the NPC (Folkmann *et al.*, 2013).

Second, all known functions of *Gle1* are intimately linked to the modulation of DEAD-box RNA helicases in mRNA export or translation (Alcazar-Roman *et al.*, 2006; Weirich *et al.*, 2006; Bolger *et al.*, 2008; Bolger and Wenthe, 2011). Given that perturbations on centrosomes are independent of defects in nuclear mRNA export (Figure 3), *Gle1* might regulate unknown DEAD-box protein(s) and a subset of mRNAs at the centrosome. Of interest, a global analysis of mRNA localization shows that the transcript of *Drosophila* pericentrin-like

gene *CP309/PLP* is localized to the centrosome (Lecuyer *et al.*, 2007). Thus it is tempting to speculate that Gle1 indeed regulates the localized translation of *PCNT* mRNA and facilitates the assembly of *PCNT* into the centrosome. Alternatively, Gle1 might facilitate the trafficking of *PCNT* mRNA to the centrosome. We propose that Gle1 serves as a unique link between the modulation of centrosome function and the regulation of RNA metabolism at different subcellular compartments. As such, cellular coordination between efficient gene expression and continued cell division is potentially facilitated.

Our 3D-SIM data show that Gle1 adapts a toroid structure at the outer layer of the PCM around the mother centriole (Figure 2C and Supplemental Figure S1B). However, it is unclear how Gle1 is localized to the mother centriole. Others reported the presence of some Nups at the cilia (Kee *et al.*, 2012), and we documented human Gle1 interactions with at least two Nups, including Nup155 and hCG1 (Rayala *et al.*, 2004; Kendirgi *et al.*, 2005). Thus Gle1 might be localized to centrosomes and basal bodies via interactions with centrosome/basal body-localized Nups. Nup155 and hCG1 localization at centrosomes or basal bodies has not been reported and will be the focus of future studies. However, Nup155 interacts in a specific subcomplex with Nup93 and Nup188 (Grandi *et al.*, 1997; Hawryluk-Gara *et al.*, 2008). Of interest, a recent study demonstrated that both Nup93 and Nup188 are localized at centrosomes and basal bodies and are required for ciliary function (Del Viso *et al.*, 2016). We propose that Nup155 is part of the Nup93/Nup188 centriole/basal body complex and provides a specific binding site for Gle1.

Given the role of Gle1 in cilia and centrosomes, it is noteworthy that LCCS1, the congenital disorder caused by mutations in human Gle1, does not have clinical features similar to ciliopathies (Herva *et al.*, 1985, 1988; Vuopala and Herva, 1994; Nousiainen *et al.*, 2008). The lack of ciliopathy phenotypes could be due to the fact that Gle1 plays essential roles outside of centrosomes/cilia (e.g., in mRNA export). Indeed, in our prior studies, we linked the LCCS1 mutant allele (Gle1-Fin<sup>Major</sup>) to altered Gle1 function at the nuclear pore complex during mRNA export (Folkman *et al.*, 2013). Thus the pleiotropic LCCS1 effects upon the loss or alteration of Gle1 might mask the ciliopathy phenotypes, which would have been observed otherwise if the defects were more restricted to only centrosomes and cilia.

Regarding the disease mechanisms underlying LCCS1 in neural precursor death in the zebrafish model of LCCS1 (Jao *et al.*, 2012), the results in this study highlight the importance of considering the effect of Gle1 deficiency on centrosome/ciliary function and whether some of the pathological features are the result of centrosome/ciliary dysfunction during neurogenesis. Concordant with this notion, during neurogenesis in many different biological systems, ciliary structures of neural precursors undergo remarkable remodeling events, such as asymmetric inheritance of ciliary remnants (Paridaen *et al.*, 2013), differential positioning of cilia (Wilsch-Brauninger *et al.*, 2012), and abrupt abscission of ciliary membranes (Das and Storey, 2014). Determining whether Gle1 dysfunction affects any of these events involving plasticity of ciliary structures during neurogenesis may shed new light on the disease pathology caused by Gle1 dysfunction.

In sum, Gle1 is another unique “moonlighting” factor (e.g., Madarampalli *et al.*, 2015) that plays important roles in centrosome/basal body function independent from its roles at the NPC in mRNA export. This work suggests that local regulation of RNA metabolism at the centrosome and basal body is a potential new layer of control in centrosome function and ciliary signaling. With the intimate connection between Gle1 and components of the inositol signaling *Ipk1/IP<sub>6</sub>* and the importance of inositol pathways in cell and developmental signaling (Bielas *et al.*, 2009; Sarmah and Wenthe, 2010;

Xu *et al.*, 2016), an exciting future challenge is to further elucidate the interplay between RNA metabolism, Gle1, and inositol signaling at the centrosome and basal body.

## MATERIALS AND METHODS

### Zebrafish husbandry

Wild-type AB and *Tg(-5.1mnx1:TagRFP)* fish were bred and maintained using standard procedures (Westerfield, 2000). Embryos were obtained by natural spawning and staged as described (Kimmel *et al.*, 1995). All animal research was approved by the Institutional Animal Care and Use Committee, Office of Animal Welfare Assurance, Vanderbilt University.

### Plasmids and RNA synthesis

The coding sequences of zebrafish *arl13b* and *centrin4* (*cetn4*) were amplified from total RNA by reverse transcriptase PCR as described (Jao *et al.*, 2012) and cloned into a Gateway Entry vector (Kwan *et al.*, 2007). The plasmids with *arl13b*-eGFP, *cetn4*-TagRFP, and eGFP-GLE1, under the control of the CMV/SP6 promoter, were generated by MultiSite Gateway cloning (Kwan *et al.*, 2007; Jao *et al.*, 2012). For *arl13b*-eGFP and *cetn4*-TagRFP RNA, the template DNA was linearized by NotI digestion and purified using a QIAprep column (Qiagen, Germantown, MD). Capped RNA was synthesized using an mMESSAGE mMACHINE SP6 kit (Invitrogen, Grand Island, NY) and purified using an RNeasy Mini kit (Qiagen) following manufacturers' instructions.

### Microinjections

Antisense morpholino oligonucleotides (MOs) and RNA were microinjected as described (Jao *et al.*, 2012). Briefly, one-cell-stage embryos from wild-type or *Tg(-5.1mnx1:TagRFP)* fish were injected with ~1 nl of MOs or RNA. To label the cilia and centrosomes in early zebrafish embryos, ~30 pg of *arl13b*-eGFP and *cetn4*-TagRFP RNA were injected into one-cell-stage embryos. To knock down *ipk1* and *gle1*, translation-blocking *ipk1* morpholino (*ipk1*<sup>MO1</sup>; Sarmah *et al.*, 2005) and a mix of *drgle1*ATG1 MO and *drgle1*UTR1 MO (*gle1*<sup>MOs</sup>; Jao *et al.*, 2012) were injected, respectively, at suboptimal doses (4 ng/embryo for *ipk1*<sup>MO1</sup> and 1.5 ng each/embryo for *gle1*<sup>MOs</sup>). The direction of heart looping was assessed at 60–72 h postfertilization as described (Sarmah *et al.*, 2005) in the *Tg(-5.1mnx1:TagRFP)* embryos, where their hearts were fluorescently labeled with TagRFP.

### Cell culture, siRNA, and transfection

The hTERT-immortalized retinal pigment epithelial cell line (RPE-1; a gift from Irina Kaverina, Vanderbilt University, Nashville, TN) and CETN-GFP RPE-1 cells (a gift from Alexey Khodjakov, Wadsworth Center, New York State Department of Health, Rensselaer Polytechnic Institute, Albany, NY; Uetake *et al.*, 2007) were maintained in DMEM/F12 and U-2 OS cells in DMEM. All cells were supplemented with 10% fetal bovine serum (FBS) and maintained in a humidified incubator at 37°C in 5% CO<sub>2</sub>. To induce ciliogenesis in Figure 1B, cells were grown in DMEM/F12 with 0.5% FBS for 48 h. For siRNA transfection, cells were transfected with 40 nM scrambled control siRNA, *GLE1* siRNA (Predesigned siRNA from Qiagen; Hs\_GLE1L\_4 FlexiTube siRNA, and Hs\_GLE1L\_7 FlexiTube siRNA), or 20 nM *NXF1* siRNA (GE Dharmacon, Lafayette, CO), using DharmaFECT 1 transfection reagent (GE Dharmacon) and following the manufacturer's instructions. siRNA-transfected cells were analyzed 72 h posttransfection.

### Antibodies

Guinea pig anti-human Gle1 antibody (1:300, ASW48) was previously reported (Aditi *et al.*, 2015). Rabbit anti-CETN antibody



(1:1500; Gayek and Ohi, 2014) was a gift from Ryoma Ohi (Vanderbilt University, Nashville, TN). The following antibodies were purchased commercially: rabbit anti-Gle1 (1:300, ab96007; Abcam, Cambridge, MA; target region, amino acids 414–656), rabbit anti-PCNT (1:500; ab4448; Abcam), rabbit anti-NIN (1:500, ab4447; Abcam), mouse anti- $\gamma$ -tubulin (1:300; GTU-88; Sigma-Aldrich), rat anti- $\alpha$ -tubulin (1:500; YOL1/34; Accurate Chemical, Westbury, NY), mouse anti- $\beta$ -actin (1:10,000; A5441; Sigma-Aldrich, St. Louis, MO), and rabbit anti-glyceraldehyde-3-phosphate dehydrogenase (1:1000, 2118L; Cell Signaling Technology, Danvers, MA). Secondary antibodies were Alexa Fluor 488, 568, or 647 (1:400; Invitrogen).

### Immunofluorescence

Cells grown on coverslips were fixed in ice-cold methanol at  $-20^{\circ}\text{C}$  for 5 min or 4% paraformaldehyde (for rabbit anti-Gle1 antibody), rinsed in 1 $\times$  phosphate-buffered saline (PBS) briefly, and incubated in blocking solution (2% goat serum, 0.1% Triton X-100, and 10 mg/ml of bovine serum albumin in 1 $\times$  PBS) at room temperature for 1 h. Primary antibodies were diluted in blocking solution and incubated at room temperature for 1 h. After washes with 1 $\times$  PBS, the cells were incubated with secondary antibodies for 1 h. Nuclei were counterstained with 1  $\mu\text{M}$  TO-PRO-3 dye (Invitrogen). Coverslips were mounted using Vectashield HardSet mounting medium (Vector Labs, Burlingame, CA).

### Microscopy

Confocal microscopy was performed using a Leica TCS SP5 laser-scanning confocal microscope equipped with a 100 $\times$ /numerical aperture (NA) 1.47 HCX PL APO oil-immersion objective. Images were processed using LAS AF (Leica, Wetzlar, Germany) and ImageJ (National Institutes of Health, Bethesda, MD) software. Superresolution microscopy was performed using a 3D-SIM system (OMX v.4; Applied Precision/GE Healthcare, Marlborough, MA) equipped with a 60 $\times$ /NA 1.45 Plan-Apochromat oil-immersion objective (Olympus, Tokyo, Japan). The 3D image stacks (0.125  $\mu\text{m}$  apart) were captured with sequential excitation of fluorophores and reconstructed using the softWoRx 5.0 software package (Applied Precision) with the following parameters: Wiener filter constant, 0.001; background intensity offset, 50.00; and custom k0 angles. For final display of cropped centrosomal regions, 3D-SIM micrographs were further resampled (6 $\times$  Preserve Detail algorithm, Photoshop CC; Adobe, San Jose, CA). Brightness and contrast were adjusted using Photoshop CC in accordance with journal policy. Figures were composed with Adobe Illustrator CC.

### Oligo-dT in situ hybridization

Cells were incubated with 1 ng/ $\mu\text{l}$  Cy3-labeled 50mer oligo-dT DNA in hybridization buffer containing 125  $\mu\text{g}/\text{ml}$  tRNA, 1 mg/ml single-stranded DNA, 1% bovine serum albumin, 10% dextran sulfate, 50% formamide, and 5 $\times$  saline sodium citrate (SSC; 0.75 M sodium chloride and 75 mM sodium citrate, pH 7.0) at  $37^{\circ}\text{C}$  for 1.5 h, followed by washes with 2 $\times$  SSC (5 min  $\times$  2 at room temperature) and 1 $\times$  PBS (10 min  $\times$  2 at room temperature) before mounting. For cells subjected to both antibody staining and in situ hybridization, immunofluorescence was performed first.

### Microtubule regrowth assays

Cells were chilled on ice for 50 min and then recovered at  $30^{\circ}\text{C}$ . At various time points after recovery, cells were fixed and permeabilized in 4% paraformaldehyde, 0.1% glutaraldehyde, and 0.2% Triton X-100 in 1 $\times$  PBS for 15 min before the immunofluorescence procedure.

### ACKNOWLEDGMENTS

We thank the Wentz laboratory for discussions, Irina Kaverina for the RPE-1 cells, Alexey Khodjakov for the CETN-GFP RPE-1 stable cell line, and Ryoma Ohi for anti-CETN antibody. Experiments were performed in part through the use of the VUMC Cell Imaging Shared Resource (supported by National Institutes of Health Grants CA68485, DK20593, DK58404, DK59637, and EY08126). This work was supported by the March of Dimes Foundation (FY-10-360 to S.R.W.) and the National Institutes of Health (5R37GM051219 to S.R.W.).

### REFERENCES

- Aditi, Folkmann AW, Wentz SR (2015). Cytoplasmic hGle1A regulates stress granules by modulation of translation. *Mol Biol Cell* 26, 1476–1490.
- Alcazar-Roman AR, Bolger TA, Wentz SR (2010). Control of mRNA export and translation termination by inositol hexakisphosphate requires specific interaction with Gle1. *J Biol Chem* 285, 16683–16692.
- Alcazar-Roman AR, Tran EJ, Guo S, Wentz SR (2006). Inositol hexakisphosphate and Gle1 activate the DEAD-box protein Dbp5 for nuclear mRNA export. *Nat Cell Biol* 8, 711–716.
- Anderson RG (1972). The three-dimensional structure of the basal body from the rhesus monkey oviduct. *J Cell Biol* 54, 246–265.
- Bielas SL, Silhavy JL, Brancati F, Kisseleva MV, Al-Gazali L, Sztrihai L, Bayoumi RA, Zaki MS, Abdel-Aleem A, Rosti RO, et al. (2009). Mutations in INPP5E, encoding inositol polyphosphate-5-phosphatase E, link phosphatidyl inositol signaling to the ciliopathies. *Nat Genet* 41, 1032–1036.
- Bolger TA, Folkmann AW, Tran EJ, Wentz SR (2008). The mRNA export factor Gle1 and inositol hexakisphosphate regulate distinct stages of translation. *Cell* 134, 624–633.
- Bolger TA, Wentz SR (2011). Gle1 is a multifunctional DEAD-box protein regulator that modulates Ded1 in translation initiation. *J Biol Chem* 286, 39750–39759.
- Bornens M (2002). Centrosome composition and microtubule anchoring mechanisms. *Curr Opin Cell Biol* 14, 25–34.
- Boveri T (1900). Über die Natur der Centrosomen. *Zellen-Studien* 4, Jena, Germany: G. Fischer.
- Dammermann A, Muller-Reichert T, Pelletier L, Habermann B, Desai A, Oegema K (2004). Centriole assembly requires both centriolar and pericentriolar material proteins. *Dev Cell* 7, 815–829.
- Das RM, Storey KG (2014). Apical abscission alters cell polarity and dismantles the primary cilium during neurogenesis. *Science* 343, 200–204.
- Del Viso F, Huang F, Myers J, Chalfant M, Zhang Y, Reza N, Bewersdorff J, Lusk CP, Khokha MK (2016). Congenital heart disease genetics uncovers context-dependent organization and function of nucleoporins at cilia. *Dev Cell* 38, 478–492.
- Dictenberg JB, Zimmerman W, Sparks CA, Young A, Vidair C, Zheng Y, Carrington W, Fay FS, Dosssey SJ (1998). Pericentriolar and gamma-tubulin form a protein complex and are organized into a novel lattice at the centrosome. *J Cell Biol* 141, 163–174.
- Dosssey S (2001). Re-evaluating centrosome function. *Nat Rev Mol Cell Biol* 2, 688–698.
- Essner JJ, Amack JD, Nyholm MK, Harris EB, Yost HJ (2005). Kupffer's vesicle is a ciliated organ of asymmetry in the zebrafish embryo that initiates left-right development of the brain, heart and gut. *Development* 132, 1247–1260.
- Folkmann AW, Collier SE, Zhan X, Aditi, Ohi MD, Wentz SR (2013). Gle1 functions during mRNA export in an oligomeric complex that is altered in human disease. *Cell* 155, 582–593.
- Fu J, Glover DM (2012). Structured illumination of the interface between centriole and peri-centriolar material. *Open Biol* 2, 120104.
- Gayek AS, Ohi R (2014). Kinetochore-microtubule stability governs the metaphase requirement for Eg5. *Mol Biol Cell* 25, 2051–2060.
- Gould RR, Borisy GG (1977). The pericentriolar material in Chinese hamster ovary cells nucleates microtubule formation. *J Cell Biol* 73, 601–615.
- Grandi P, Dang T, Pane N, Shevchenko A, Mann M, Forbes D, Hurt E (1997). Nup93, a vertebrate homologue of yeast Nic96p, forms a complex with a novel 205-kDa protein and is required for correct nuclear pore assembly. *Mol Biol Cell* 8, 2017–2038.
- Hawryluk-Gara LA, Platani M, Santarella R, Wozniak RW, Mattaj JW (2008). Nup53 is required for nuclear envelope and nuclear pore complex assembly. *Mol Biol Cell* 19, 1753–1762.



- Herva R, Conradi NG, Kalimo H, Leisti J, Sourander P (1988). A syndrome of multiple congenital contractures: neuropathological analysis on five fetal cases. *Am J Med Genet* 29, 67–76.
- Herva R, Leisti J, Kirkinen P, Seppanen U (1985). A lethal autosomal recessive syndrome of multiple congenital contractures. *Am J Med Genet* 20, 431–439.
- Jao LE, Appel B, Wente SR (2012). A zebrafish model of lethal congenital contracture syndrome 1 reveals Gle1 function in spinal neural precursor survival and motor axon arborization. *Development* 139, 1316–1326.
- Kaneb HM, Folkmann AW, Belzil VV, Jao LE, Leblond CS, Girard SL, Daoud H, Noreau A, Rochefort D, Hince P, et al. (2015). Deleterious mutations in the essential mRNA metabolism factor, hGle1, in amyotrophic lateral sclerosis. *Hum Mol Genet* 24, 1363–1373.
- Kang Y, Cullen BR (1999). The human Tap protein is a nuclear mRNA export factor that contains novel RNA-binding and nucleocytoplasmic transport sequences. *Genes Dev* 13, 1126–1139.
- Kee HL, Dishinger JF, Blasius TL, Liu CJ, Margolis B, Verhey KJ (2012). A size-exclusion permeability barrier and nucleoporins characterize a ciliary pore complex that regulates transport into cilia. *Nat Cell Biol* 14, 431–437.
- Kendirgi F, Barry DM, Griffis ER, Powers MA, Wente SR (2003). An essential role for hGle1 nucleocytoplasmic shuttling in mRNA export. *J Cell Biol* 160, 1029–1040.
- Kendirgi F, Rexer DJ, Alcazar-Roman AR, Onishko HM, Wente SR (2005). Interaction between the shuttling mRNA export factor Gle1 and the nucleoporin hCG1: a conserved mechanism in the export of Hsp70 mRNA. *Mol Biol Cell* 16, 4304–4315.
- Khodjakov A, Cole RW, Oakley BR, Rieder CL (2000). Centrosome-independent mitotic spindle formation in vertebrates. *Curr Biol* 10, 59–67.
- Kimmel CB, Ballard WW, Kimmel SR, Ullmann B, Schilling TF (1995). Stages of embryonic development of the zebrafish. *Dev Dyn* 203, 253–310.
- Kodani A, Salome Sierol-Piquer M, Seol A, Garcia-Verdugo JM, Reiter JF (2013). Kif3a interacts with Dynactin subunit p150 Glued to organize centriole subdistal appendages. *EMBO J* 32, 597–607.
- Kunimoto K, Yamazaki Y, Nishida T, Shinohara K, Ishikawa H, Hasegawa T, Okanou T, Hamada H, Noda T, Tamura A, et al. (2012). Coordinated ciliary beating requires Odf2-mediated polarization of basal bodies via basal feet. *Cell* 148, 189–200.
- Kwan KM, Fujimoto E, Grabher C, Mangum BD, Hardy ME, Campbell DS, Parant JM, Yost HJ, Kanki JP, Chien CB (2007). The Tol2kit: a multisite gateway-based construction kit for Tol2 transposon transgenesis constructs. *Dev Dyn* 236, 3088–3099.
- Lawo S, Hasegan M, Gupta GD, Pelletier L (2012). Subdiffraction imaging of centrosomes reveals higher-order organizational features of pericentriolar material. *Nat Cell Biol* 14, 1148–1158.
- Lecuyer E, Yoshida H, Parthasarathy N, Alm C, Babak T, Cerovina T, Hughes TR, Tomancak P, Krause HM (2007). Global analysis of mRNA localization reveals a prominent role in organizing cellular architecture and function. *Cell* 131, 174–187.
- Lee HS, Lee DH, Cho HK, Kim SH, Auh JH, Pai HS (2015). InsP6-sensitive variants of the Gle1 mRNA export factor rescue growth and fertility defects of the ipk1 low-phytic-acid mutation in Arabidopsis. *Plant Cell* 27, 417–431.
- Loncarek J, Hergert P, Magidson V, Khodjakov A (2008). Control of daughter centriole formation by the pericentriolar material. *Nat Cell Biol* 10, 322–328.
- Madarampalli B, Yuan Y, Liu D, Lengel K, Xu Y, Li G, Yang J, Liu X, Lu Z, Liu DX (2015). ATF5 connects the pericentriolar materials to the proximal end of the mother centriole. *Cell* 162, 580–592.
- Martinez-Campos M, Basto R, Baker J, Kernan M, Raff JW (2004). The Drosophila pericentrin-like protein is essential for cilia/flagella function, but appears to be dispensable for mitosis. *J Cell Biol* 165, 673–683.
- Mennella V, Keszthelyi B, McDonald KL, Chhun B, Kan F, Rogers GC, Huang B, Agard DA (2012). Subdiffraction-resolution fluorescence microscopy reveals a domain of the centrosome critical for pericentriolar material organization. *Nat Cell Biol* 14, 1159–1168.
- Montpetit B, Thomsen ND, Helmke KJ, Seeliger MA, Berger JM, Weis K (2011). A conserved mechanism of DEAD-box ATPase activation by nucleoporins and InsP6 in mRNA export. *Nature* 472, 238–242.
- Moritz M, Braunfeld MB, Guenebaut V, Heuser J, Agard DA (2000). Structure of the gamma-tubulin ring complex: a template for microtubule nucleation. *Nat Cell Biol* 2, 365–370.
- Moser JJ, Fritzler MJ, Ou Y, Rattner JB (2010). The PCM-basal body/primary cilium coalition. *Semin Cell Dev Biol* 21, 148–155.
- Nakagawa Y, Yamane Y, Okanou T, Tsukita S, Tsukita S (2001). Outer dense fiber 2 is a widespread centrosome scaffold component preferentially associated with mother centrioles: its identification from isolated centrosomes. *Mol Biol Cell* 12, 1687–1697.
- Nigg EA (2002). Centrosome aberrations: cause or consequence of cancer progression? *Nat Rev Cancer* 2, 815–825.
- Nousiainen HO, Kestila M, Pakkasjarvi N, Honkala H, Kuure S, Tallila J, Vuopala K, Ignatius J, Herva R, Peltonen L (2008). Mutations in mRNA export mediator GLE1 result in a fetal motoneuron disease. *Nat Genet* 40, 155–157.
- Paridaen JT, Wilsch-Brauninger M, Huttner WB (2013). Asymmetric inheritance of centrosome-associated primary cilium membrane directs ciliogenesis after cell division. *Cell* 155, 333–344.
- Rayala HJ, Kendirgi F, Barry DM, Majerus PW, Wente SR (2004). The mRNA export factor human Gle1 interacts with the nuclear pore complex protein Nup155. *Mol Cell Proteomics* 3, 145–155.
- Rieder CL, Borisy GG (1982). The centrosome cycle in PtK2 cells: asymmetric distribution and structural changes in the pericentriolar material. *Biol Cell* 44, 117–132.
- Sarmah B, Latimer AJ, Appel B, Wente SR (2005). Inositol polyphosphates regulate zebrafish left-right asymmetry. *Dev Cell* 9, 133–145.
- Sarmah B, Wente SR (2010). Zebrafish inositol polyphosphate kinases: new effectors of cilia and developmental signaling. *Adv Enzyme Regul* 50, 309–323.
- Sarmah B, Winfrey VP, Olson GE, Appel B, Wente SR (2007). A role for the inositol kinase Ipk1 in ciliary beating and length maintenance. *Proc Natl Acad Sci USA* 104, 19843–19848.
- Sonnen KF, Schermelleh L, Leonhardt H, Nigg EA (2012). 3D-structured illumination microscopy provides novel insight into architecture of human centrosomes. *Biol Open* 1, 965–976.
- Takahashi M, Yamagiwa A, Nishimura T, Mukai H, Ono Y (2002). Centrosomal proteins CG-NAP and kendrin provide microtubule nucleation sites by anchoring gamma-tubulin ring complex. *Mol Biol Cell* 13, 3235–3245.
- Tran EJ, Zhou Y, Corbett AH, Wente SR (2007). The DEAD-box protein Dbp5 controls mRNA export by triggering specific RNA:protein remodeling events. *Mol Cell* 28, 850–859.
- Uetake Y, Loncarek J, Nordberg JJ, English CN, La Terra S, Khodjakov A, Sluder G (2007). Cell cycle progression and de novo centriole assembly after centrosomal removal in untransformed human cells. *J Cell Biol* 176, 173–182.
- Vuopala K, Herva R (1994). Lethal congenital contracture syndrome: further delineation and genetic aspects. *J Med Genet* 31, 521–527.
- Wang WJ, Soni RK, Uryu K, Tsou MF (2011). The conversion of centrioles to centrosomes: essential coupling of duplication with segregation. *J Cell Biol* 193, 727–739.
- Weirich CS, Erzberger JP, Flick JS, Berger JM, Thorner J, Weis K (2006). Activation of the DExD/H-box protein Dbp5 by the nuclear-pore protein Gle1 and its coactivator InsP6 is required for mRNA export. *Nat Cell Biol* 8, 668–676.
- Westerfield M (2000). *The Zebrafish Book. A Guide for the Laboratory Use of Zebrafish (Danio rerio)*, Eugene: University of Oregon Press.
- Wilsch-Brauninger M, Peters J, Paridaen JT, Huttner WB (2012). Basolateral rather than apical primary cilia on neuroepithelial cells committed to delamination. *Development* 139, 95–105.
- Xu Q, Zhang Y, Wei Q, Huang Y, Hu J, Ling K (2016). Phosphatidylinositol phosphate kinase PIPKgamma and phosphatase INPP5E coordinate initiation of ciliogenesis. *Nat Commun* 7, 10777.
- York JD, Odom AR, Murphy R, Ives EB, Wente SR (1999). A phospholipase C-dependent inositol polyphosphate kinase pathway required for efficient messenger RNA export. *Science* 285, 96–100.
- Zimmerman WC, Sillibourne J, Rosa J, Doherty SJ (2004). Mitosis-specific anchoring of gamma tubulin complexes by pericentriolar controls spindle organization and mitotic entry. *Mol Biol Cell* 15, 3642–3657.